ACS APPLIED MATERIALS & INTERFACES

Letter

www.acsami.org

Improved Performances in Polymer BHJ Solar Cells Through Frontier Orbital Tuning of Small Molecule Additives in Ternary Blends

Akshay Kokil,*[,†] Ambata M. Poe,[‡] Youngju Bae,[‡] Andrea M. Della Pelle,[‡] Paul J. Homnick,[‡] Paul M. Lahti,*[,‡] Jayant Kumar,*[,†] and S. Thayumanavan*[,‡]

[†]Center for Advanced Materials, University of Massachusetts Lowell, One University Avenue, Lowell, Massachusetts 01854, United States

[‡]Department of Chemistry, University of Massachusetts Amherst, 710 North Pleasant Street, Amherst, Massachusetts 01003, United States

Supporting Information

ABSTRACT: Polymer solar cells fabricated in air under ambient conditions are of significant current interest, because of the implications in practicality of such devices. However, only moderate performance has been obtained for the air-processed devices. Here, we report that enhanced short circuit current density (J_{SC}) and open circuit voltage (V_{OC}) in air-processed poly(3-hexylthiophene) (P3HT)-based solar cells can be obtained by using a series of donor−acceptor dyes as the third component in the device. Power conversion efficiencies up to 4.6% were obtained upon addition of the dyes which are comparable to high-performance P3HT solar cells fabricated in controlled environments. Multilayer planar solar cells containing interlayers of the donor−acceptor dyes, revealed that along with infrared sensitization, an energy level cascade architecture and Förster resonance energy transfer could contribute to the enhanced performance.

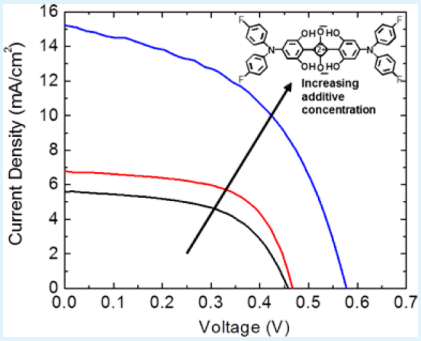

KEYWORDS: *polymer solar cells, bulk heterojunction solar cells, planar multilayer solar cells, donor−acceptor dyes*

Polymer bulk-heterojunction solar cells (PSC) offer a promising route toward lightweight, large area, flexible energy-harvesting devices, which are readily amenable to roll-to-roll high volume production.[1−3] The most widely utilized PSCs employing poly(3-hexylthiophene) (P3HT) and [6,6]-phenyl-C61-butyric acid methyl ester ($PC_{61}BM$), have yielded power conversion efficiencies (PCE) up to 5%.[4−7] The upper limit in PCE in P3HT/$PC_{61}BM$ devices could be determined by the fact that low energy absorption band edge of the active layer is limited to ∼700 nm. To address this inherent limitation with this combination, researchers have taken two promising approaches. In one approach, new generation lower band gap polymers that absorb in the red and near-infrared (NIR) have been reported and this approach has yielded PSC efficiencies approaching 9%.[8−15] In an alternate approach, use of ternary blends of P3HT with low band gap polymers has been explored.[16,17] Improved PSC performance in these cases was attributed to better light harvesting in the red and NIR regions by the ternary blends. However, a reduced external quantum efficiency was observed in the P3HT absorption region of these blends. Interestingly, it has been reported that an aliphatic amine-based squaraine additive in the P3HT/$PC_{61}BM$ active layer can lead to improved J_{SC} in the solar cell.[18] Interestingly, a constant open circuit voltage (V_{OC}) was reported, which was pinned to the lowest energy difference between the highest occupied molecular orbital (HOMO) of the P3HT donor and the lowest unoccupied molecular orbital (LUMO) of the $PC_{61}BM$ acceptor. An attractive strategy to improve the PCE in this combination will be to improve the V_{OC}. We envisaged the possibility that this can be achieved by systematically varying the redox potential of the squaraine additives. In this manuscript, we report our findings on the effect of systematically varying the frontier orbital energy levels upon the V_{OC} and the overall efficiency of squaraine-containing P3HT/$PC_{61}BM$ solar cells.

Note that most of the reported PSCs discussed above are fabricated in an oxygen- and moisture-free controlled environment. Although these controlled conditions provide the opportunity to obviate variations due to environmental variations, it is also clear that device fabrication in air under ambient conditions would lead to cheaper and high-throughput production of PSCs. However, the PSCs fabricated in air tend to display significantly reduced PCEs.[19,20] We stipulated that our devices be fabricated and tested in air under ambient conditions. We show here that efficiencies of up to 4.62% can be obtained in squaraine-based ternary blends in these air-processed devices, which are comparable to the high-performance P3HT/$PC_{61}BM$ based devices fabricated in controlled environments. The improved performance observed for devices with ternary blends, is attributed to an energy level cascade in the active layer components, with sensitization by the squaraines in red and NIR spectral regions.

Received: April 10, 2014
Accepted: June 19, 2014
Published: June 19, 2014

   dx.doi.org/10.1021/am5021759 | *ACS Appl. Mater. Interfaces* 2014, 6, 9920−9924

FIGURES.

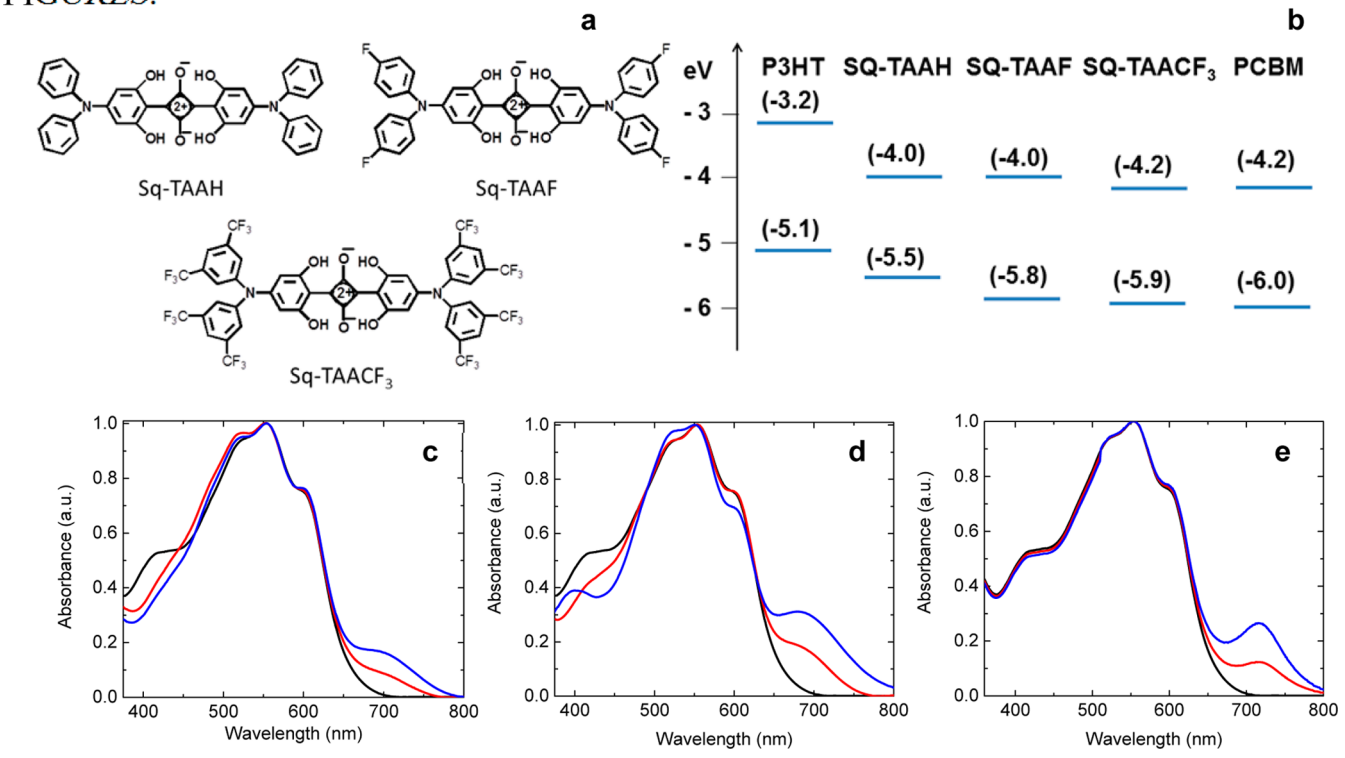

Figure 1. (a) Chemical structures of the squaraine additives. (b) Frontier molecular orbital energy levels of the utilized materials. UV−visible absorption spectra of the P3HT/$PC_{61}BM$ active layers with (c) Sq-TAAH, (d) Sq-TAAF, and (e) Sq-$TAACF_3$; P3HT/$PC_{61}BM$ (black line), 5 wt % squaraine (red line), 10 wt % squaraine (blue line).

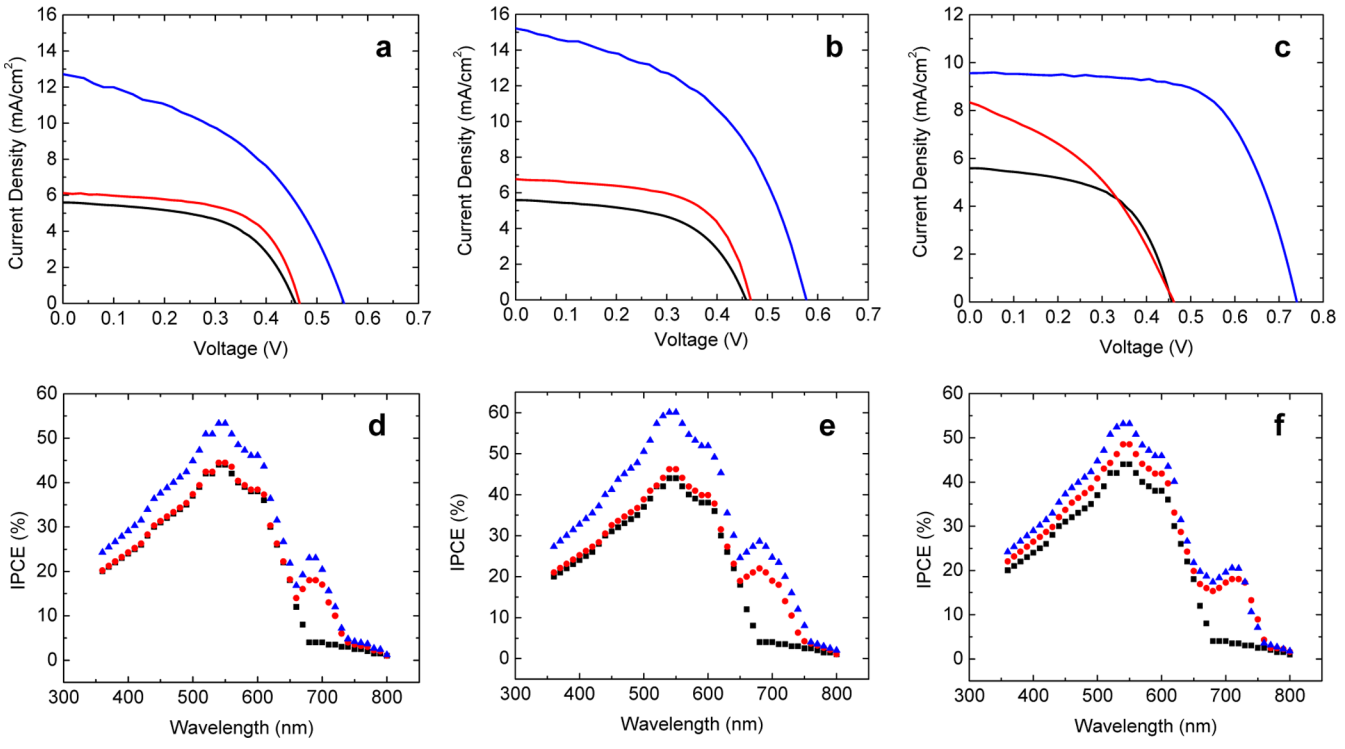

Figure 2. Current density−voltage (J−V) curves for the PSCs with (a) Sq-TAAH, (b) Sq-TAAF, and (c) Sq-$TAACF_3$; P3HT/$PC_{61}BM$ (black line), 5 wt % squaraine (red line), 10 wt % squaraine (blue line). IPCE spectra for the PSCs with (d) Sq-TAAH, (e) Sq-TAAF, and (f) Sq-$TAACF_3$; P3HT/$PC_{61}BM$ (black squares), 5 wt % squaraine (red circles), 10 wt % squaraine (blue triangles).

Squaraine dyes with aromatic amines have been reported as good light-harvesting donor materials in small molecule solar cells.[21] Additionally, the phenyl groups in the triarylamines can be readily functionalized to render the obtained dyes with well-

dx.doi.org/10.1021/am5021759 | ACS Appl. Mater. Interfaces 2014, 6, 9920−9924

tuned redox potentials.[22] The dyes employed in the ternary blend were chosen to have a "weak-donor−strong-acceptor−weak-donor" design (Figure 1a) with squaraine as the acceptor and triarylamines as donors. To investigate the effect of change in the dye frontier molecular orbital energy levels on obtained ternary blend performance, we selected triarylamines bearing electron withdrawing groups (*para*-fluoro and *meta*,*meta*-bis-trifluoromethyl) (Figure 1b).[22] Importantly, these additives were selected to have HOMO and LUMO levels lying between those of P3HT and $PC_{61}BM$, enabling an energy level cascade in the active layer (Figure 1b). The additives have high molar absorptivities (1×10^4 to 1×10^5 M^{-1} cm^{-1}) with solid state absorption maxima at 715 nm (Sq-TAAH), 706 nm (Sq-$TAACF_3$), and 687 nm (Sq-TAAF). Interestingly, the functionalized dyes also displayed different charge transport characteristics. They exhibit hole (Sq-TAAH), electron (Sq-$TAACF_3$), and ambipolar (Sq-TAAF) carrier mobilities of $\sim 1 \times 10^{-5}$ to 1×10^{-6} cm^2 V^{-1} s^{-1}, as characterized in the field effect transistor mode.[22] The squaraines were solution blended at a constant 1:1 ratio of (P3HT + Squaraine):$PC_{61}BM$, and a weight fraction of 5−10%. Device active layers were spin coated in air under ambient conditions as described in the experimental section. The complementary absorption of P3HT and the squaraine gives an active layer absorption spanning much of the solar spectrum (Figures 1c−e). The absorption of the employed squaraines also overlaps with the photoluminescence band of P3HT (see the Supporting Information, Figure S1), which enables exciton transfer from P3HT to the squaraines through FRET. From the spectra (see the Supporting Information, Figure S1), the Förster radius R_0 is estimated to be favorable at 7.5 nm for Sq-TAAH and Sq-TAAF, and 7.0 nm for Sq-$TAACF_3$.

All the PSCs used PEDOT−PSS as the electron blocking layer and Al as the cathode, with thermal annealing in a final step (see the Supporting Information, Figure S2). PSCs were characterized in air using AM 1.5 direct irradiation at 100 mW·cm^{-2} light intensity. The thickness of the active layer for all the fabricated devices was 150 nm. Device J-V curves are given in Figure 2, with the performance metrics summarized in Table 1.

Table 1. PSC Performance Characteristics

squaraine	fraction (wt %)	J_{SC} (calcd J_{SC}) ($mAcm^{-2}$)	V_{OC} (V)	FF	PCE (%)
control	0	5.6 (5.8)	0.46	0.55	1.44
Sq-TAAH	5	6.1 (6.3)	0.46	0.60	1.73
	10	12.8 (12.1)	0.55	0.42	3.10
Sq-TAAF	5	6.7 (6.5)	0.47	0.60	1.91
	10	15.2 (14.5)	0.58	0.47	4.28
Sq-$TAACF_3$	5	8.6 (8.1)	0.47	0.37	1.53
	10	9.7 (9.3)	0.73	0.65	4.62

The air-processed P3HT/$PC_{61}BM$ PSC gave a PCE of 1.44% with J_{SC} = 5.6 mA cm^{-2}, V_{OC} = 0.46 V, and 0.55 fill factor (FF); these are comparable to those of other air-processed P3HT/$PC_{61}BM$ devices.[19,20]

By comparison, PSCs with 10 wt % Sq-TAAH gave J_{SC} = 12.8 mA cm^{-2}, V_{OC} = 0.55 V, and FF = 0.42, for a 3.10% PCE (Figure 2a, Table 1). An even more striking improvement was obtained using active layers with 10% Sq-TAAF, which gave J_{SC} = 15.2 mA cm^{-2}, V_{OC} = 0.58 V with FF = 0.47 and PCE = 4.28% (Figure 2b, Table 1), which is close to some of the reported P3HT/$PC_{61}BM$ devices fabricated in controlled air and moisture free environments.[4−7] A significantly improved V_{OC} in addition to the improved J_{SC} was obtained for devices with 10 wt % Sq-$TAACF_3$ (J_{SC} = 9.7 mA cm^{-2}, V_{OC} = 0.73 V, FF = 0.65), resulting in a PCE of 4.62% (Figure 2c, Table 1), which is comparable to the high-performance P3HT/$PC_{61}BM$ PSCs discussed above. For both Sq-TAAF and Sq-$TAACF_3$, the LUMO is substantially stabilized in comparison to Sq-TAAH (Figure 1b), to be slightly higher than the LUMO of $PC_{61}BM$. Hence, high PCEs for devices with electron-poor Sq-TAAF and Sq-$TAACF_3$ could be attributed at least partly to their ambipolar and n-type charge transport characteristics, respectively.

To investigate the factors that result in the enhanced performance for ternary blends, we measured the incident photon-to-current efficiency (IPCE) spectra for the PSCs. In all cases, the devices with ternary blends (Figure 2d−f) display two prominent peaks, centered around 550 nm and around 690−715 nm, corresponding to the light harvested by P3HT and squaraines, respectively. This indicates that the squaraines actively contribute to the energy harvesting in the red and NIR region by the ternary blends. Significantly more energy is harvested upon increasing the squaraine fraction as indicated by the enhancement in IPCE peaks, resulting in an improved J_{SC}. The calculated J_{SC} values from IPCE spectra were close to the device J_{SC} (see Table 1 and the Supporting Information). Note that in all three devices, addition of 5 wt % squaraine does not afford significant enhancements in IPCE in the P3HT region, suggesting that the observed enhancement primarily arises from sensitization of the active layer in the lower energy region where the squaraines absorb. Interestingly, increasing the additive amount from 5% to 10% results in enhanced IPCE in both P3HT and squaraine absorption regimes. This could be attributed to the change in morphology, where the additives result in a morphology that facilitates exciton splitting at the interfaces. However, atomic force microscopy (AFM) performed on the active layers with squaraines did not show significant changes in the surface morphology (see the Supporting Information, Figure S1).

We were interested in further investigating the reason for increase in the IPCE peak for P3HT with increasing squaraine fraction. It has been recently reported that the photoluminescence of a squaraine derivative improved by addition of P3HT, with a concomitant reduction in the P3HT excited state lifetime.[18] By analogy, an increase in P3HT light harvesting could occur by the transfer of P3HT excitons to the additives through FRET. This could effectively increase the distance over which the exciton can migrate, resulting in improved J_{SC}. But, this would need the additive to be at the interface of P3HT and $PC_{61}BM$ phases.

To determine whether FRET can indeed contribute to the increased light harvesting in the bulk heterojunction PSCs, if the squaraines were to be at the interface between the P3HT and the fullerene phases, multilayer planar PSCs with squaraine interlayers were fabricated in air under ambient conditions. These PSCs also employed PEDOT−PSS as the electron blocking layer and Al as the cathode. To preserve the multilayer architecture, the planar PSCs were not annealed. Solubility of the squaraines in dichloromethane (DCM, a nonsolvent for P3HT) allowed spin-coating of squaraine interlayers atop the P3HT layer (see the Supporting Information, Figure S2). The P3HT layers (70 nm) were made much thicker than the squaraine layers (20 nm), to ensure a majority of light absorption in the P3HT layer. C_{60} acceptor layers were vapor deposited onto the P3HT layer for the control device and squaraine interlayer for the multilayer device. It has been reported that thermal evaporation

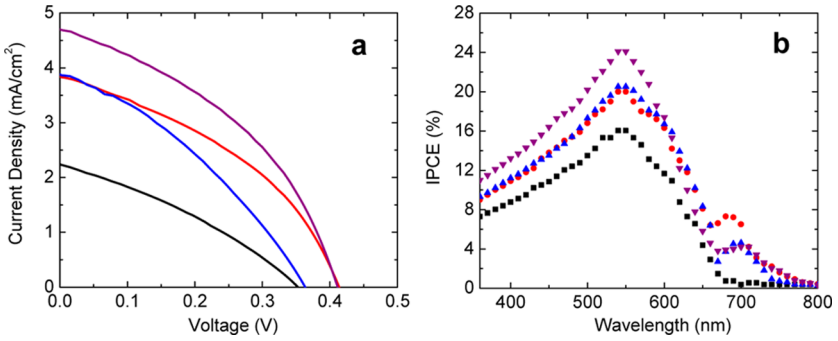

Figure 3. (a) Current density−voltage (J−V) curves for multilayer planar PSCs, P3HT/C_{60} (black line), P3HT/Sq-TAAH/C_{60} (blue line), P3HT/Sq-TAAF/C_{60} (red line), and P3HT/Sq-TAACF$_3$/C_{60} (purple line). (b) IPCE spectra for multilayer planar PSCs, P3HT/C_{60} (black squares), P3HT/Sq-TAAH/C_{60} (blue triangles), P3HT/Sq-TAAF/C_{60} (red circles), and P3HT/Sq-TAACF$_3$/C_{60} (purple inverted triangles).

of C_{60} onto P3HT does not result in a significant diffusion of the fullerene into the polymer.[23] We have replaced $PC_{61}BM$ with C_{60} because of the thermal deposition capabilities available in the latter material. The energy level cascade architecture should not be affected by this change, since the HOMO and LUMO of C_{60} are lower than those of $PC_{61}BM$. The planar devices were characterized in air using AM 1.5 direct irradiation at 100 mW cm^{-2} light intensity, with J−V curves shown in Figure 3a and performance metrics summarized in Table 2. A control device was fabricated by spin-coating "blank" solvent DCM over a dried P3HT film before vapor deposition of the C_{60} layer.

Table 2. Multilayer Planar PSC Performance Characteristics

	control P3HT/C60	P3HT/Sq-TAAH/C60	P3HT/Sq-TAAF/C60	P3HT/Sq-TAACF3/C60
J_{SC} (mA cm^{-2})	2.3	3.9	3.9	4.7
V_{OC} (V)	0.35	0.36	0.42	0.41
FF	0.30	0.33	0.37	0.39
PCE (%)	0.26	0.49	0.63	0.79

The P3HT/C_{60} bilayer PSC had a PCE = 0.26%, with J_{SC} = 2.3 mA cm^{-2}, V_{OC} = 0.35 V, and FF = 0.30. For the P3HT/Sq-TAAH/C_{60} planar PSC, J_{SC} improved significantly, whereas V_{OC} and FF increased slightly, giving an improved PCE = 0.49%. Interestingly, compared to the control, the introduction of Sq-TAAF and Sq-TAACF$_3$ interlayers strongly enhanced PCE of the planar devices with a PCE = 0.63% and PCE = 0.79%, respectively, aided by considerable improvements in the J_{SC} and V_{OC}. AFM performed on each fabricated layer suggest that the integrity of all the layers was preserved during processing (see the Supporting Information, Figure S2).

IPCE spectra for the planar multilayer PSCs are displayed in Figure 3b. As observed with the bulk-heterojunction PSCs, two distinct peaks from absorption by P3HT and squaraine were observed, but the contribution for light harvested by squaraine was considerably lower for the planar devices. Importantly, all planar PSCs with squaraine interlayers showed increased P3HT IPCE intensities. Because AFM showed the retained integrity of individual layers during processing, a donor−acceptor interface is presumably only present between the squaraine interlayer and C_{60} for the majority of the exciton separation to occur. Thus, the improved P3HT IPCE unambiguously demonstrates that FRET contributes to enhancement of the device J_{SC}. Also, the IPCE behavior for squaraine indicates red and NIR sensitization.

In general, introduction of the triarylamine containing squaraines in P3HT/$PC_{61}BM$ devices results in enhanced solar cell efficiencies for PSCs fabricated in air under ambient conditions. This PSC performance enhancement can be attributed to FRET, as the evidence from the multilayer device suggests. However, these results do not necessarily rule out an electronic cascade aiding the efficient exciton dissociation. This is particularly relevant in these studies, because the squaraines with electron withdrawing groups (Sq-TAAF and Sq-TAACF$_3$) have lower LUMOs than P3HT, which should favor a cascade electron transfer. Such a cascade could also aid the exciton dissociation in the multilayer PSC devices. Overall, the improved V_{OC} observed for both bulk heterojunction and multilayer planar PSCs in the present study indicate reduced recombination losses at squaraine/$PC_{61}BM$ interfaces.[24−27] With reduced recombination, photocurrrent can be collected over a broader voltage bias range, presumably leading to a overall higher V_{OC} as discussed[27] elsewhere. The red and NIR abosorbing squaraine dyes in a ternary blend with P3HT and $PC_{61}BM$ lead to a greatly improved absorption bandwidth in the active layer. Importantly, the added dyes improve the exciton migration in the active layer through FRET as well as the exciton dissociation due to the cascade energy levels. These factors lead to an improved light harvestation as indicated by the increased IPCE in the P3HT region, and thus result in the improved J_{SC}. A higher weight fraction of fluorine functionalized squaraines display an enhanced performance as compared to the unfunctionalized analogue, indicating that development of a suitable morphology for efficient exction dissociation is vital. Although determination of the location of the dyes in the ternary blend is a challenge, the multilayer planar devices indicate that presence of squaraine at the interface between P3HT and PCBM in the ternary blend could account for the improved PSC performance. Thus, systematic tailoring of the additive structures for well-matched frontier molecular orbital energy levels giving cascade electronic behavior is crucial for improving multiple aspects of photovoltaic performance.

In summary, we report a strategy for obtaining marked improvement in PSC performance, not just through improved device J_{SC} but also enhanced V_{OC}, through the use of ternary blends of P3HT:donor−acceptor dyes:$PC_{61}BM$. These ternary blends seem to provide morphologies with the dyes at the interface between the major electron donor and major electron acceptor, which aid in improving the exciton migration and exciton dissociation through energy transfer and electron transfer processes, respectively. Because these dye molecules are small in size, it is reasonable to imagine that frontier molecular orbital energy level tuning through electron-withdrawing or electron-donating substituents will favorably alter the V_{OC} with minimal

dx.doi.org/10.1021/am5021759 | ACS Appl. Mater. Interfaces 2014, 6, 9920−9924

effect on morphology. The hypothesis that the dyes are present at the interface has been supported by indirectly testing whether multilayer configuration devices with the dye molecules at the interface would lead to increased PCE. Overall, we believe that frontier orbital energy level tuning in small molecules to optimize the PSC performance is a useful tool in the arsenal that one needs to develop practical organic solar cells.

■ ASSOCIATED CONTENT

Supporting Information

The experimental details and AFM phase images for both bulk heterojunction and multilayer planar PSCs are presented. This material is available free of charge via the Internet at http://pubs.acs.org.

■ AUTHOR INFORMATION

Corresponding Authors

*E-mail: Akshay_Kokil@uml.edu.
*E-mail: lahti@chem.umass.edu.
*E-mail: Jayant_Kumar@uml.edu.
*E-mail: thai@chem.umass.edu.

Notes

The authors declare no competing financial interest.

■ ACKNOWLEDGMENTS

This material is based upon work supported as part of Polymer-Based Materials for Harvesting Solar Energy, an Energy Frontier Research Center funded by the U.S. Department of Energy, Office of Science, Office of Basic Energy Sciences under Award DE-SC0001087.

■ REFERENCES

(1) Thompson, B. C.; Fréchet, J. M. J. Polymer − Fullerene Composite Solar Cells. *Angew. Chem., Int. Ed.* **2008**, *47*, 58−77.

(2) Li, G.; Zhu, R.; Yang, Y. Polymer Solar Cells. *Nat. Photonics* **2012**, *6*, 153−161.

(3) Nagarjuna, G.; Venkataraman, D. Strategies For Controlling the Active Layer Morphologies in OPVs. *J. Poly. Sci. B Poly. Phys.* **2012**, *50*, 1045−1056.

(4) Chen, D.; Nakahara, A.; Wei, D.; Norlund, D.; Russell, T. P. P3HT/PCBM Bulk Heterojunction Organic Photovoltaics: Correlating Efficiency and Morphology. *Nano Lett.* **2011**, *11*, 561−567.

(5) Kim, Y.; Cook, S.; Tuladhar, S. M.; Choulis, S. A.; Nelson, J.; Durrant, J. R.; Bradley, D. D. C.; Giles, M.; McCulloch, I.; Ha, C. S.; Ree, M. A Strong Regioregularity Effect in Self-Organizing Conjugated Polymer Films and High-Efficiency Polythiophene:Fullerene Solar Cells. *Nat. Mater.* **2006**, *5*, 197−203.

(6) Li, G.; Shrotriya, V.; Huang, J.; Yao, Y.; Moriarty, T.; Emery, K.; Yang, Y. High-Efficiency Solution Processable Polymer Photovoltaic Cells by Self-Organization of Polymer Blends. *Nat. Mater.* **2005**, *4*, 864−868.

(7) Ma, W.; Yang, C.; Gong, X.; Lee, K.; Heeger, A. J. Thermally Stable, Efficient Polymer Solar Cells with Nanoscale Control of the Interpenetrating Network Morphology. *Adv. Mater.* **2005**, *15*, 1617−1622.

(8) He, Z.; Zhong, C.; Su, S.; Xu, M.; Wu, H.; Cao, Y. Enhanced Power-Conversion Efficiency in Polymer Solar Cells using an Inverted Device Structure. *Nat. Photonics* **2012**, *6*, 591−595.

(9) Choi, H.; Lee, J. P.; Ko, S. J.; Jung, J. W.; Park, H.; Yoo, S.; Park, O.; Jeong, J. R.; Park, S.; Kim, J. Y. Multipositional Silica-Coated Silver Nanoparticles for High-Performance Polymer Solar Cells. *Nano Lett.* **2013**, *13*, 2204−2208.

(10) Guo, X.; Zhou, N.; Lou, S. J.; Smith, J.; Tice, D. B.; Hennek, J. W.; Ortiz, R. P.; López Navarrete, J. T.; Li, S.; Strzalka, J.; Chen, L. X.; Chang, R. P. H.; Facchetti, A.; Marks, T. J. Polymer Solar Cells with Enhanced Fill Factors. *Nat. Photonics* **2013**, *7*, 825−833.

(11) Chen, H. C.; Chen, Y. H.; Liu, C. C.; Chien, Y. C.; Chou, S. W.; Chou, P. T. Prominent Short-Circuit Currents of Fluorinated Quinoxaline-Based Copolymer Solar Cells with a Power Conversion Efficiency of 8.0%. *Chem. Mater.* **2012**, *24*, 4766−4772.

(12) Son, H. J.; Lu, L.; Chen, W.; Xu, T.; Zheng, T.; Carsten, B.; Strzalka, J.; Darling, S. B.; Chen, L. X.; Yu, L. Synthesis and Photovoltaic Effect in Dithieno[2,3- D:2′,3′-D′]Benzo[1,2- B:4,5- B′]Dithiophene-Based Conjugated Polymers. *Adv. Mater.* **2013**, *25*, 838−843.

(13) Huang, Y.; Guo, X.; Liu, F.; Huo, L.; Chen, Y.; Russell, T. P.; Han, C. C.; Li, Y.; Hou, J. Improving the Ordering and Photovoltaic Properties by Extending π−Conjugated Area of Electron-Donating Units in Polymers with D-A Structure. *Adv. Mater.* **2012**, *24*, 3383−3389.

(14) Chu, T. Y.; Lu, J.; Beaupré, S.; Zhang, Y.; Pouliot, J. R.; Wakim, S.; Zhou, J.; Leclerc, M.; Li, Z.; Ding, J.; Tao, Y. Bulk Heterojunction Solar Cells using Thieno[3,4-C]Pyrrole-4,6-Dione and Dithieno[3,2-B:2′,3′-D]Silole Copolymer with a Power Conversion Efficiency of 7.3%. *J. Am. Chem. Soc.* **2011**, *133*, 4250−4253.

(15) Chen, H. Y.; Hou, J.; Zhang, S.; Liang, Y.; Yang, G.; Yang, Y.; Yu, L.; Wu, Y.; Li, G. Polymer Solar Cells with Enhanced Open-Circuit Voltage and Efficiency. *Nat. Photonics* **2009**, *3*, 649−653.

(16) Ameri, T.; Min, J.; Li, N.; Machui, F.; Baran, D.; Forster, M.; Schottler, K. J.; Dolfen, D.; Scherf, U.; Brabec, C. J. Performance Enhancement of the P3HT/PCBM Solar Cells Through NIR Sensitization using a Small-Bandgap Polymer. *Adv. Energy Mater.* **2012**, *2*, 1198−1202.

(17) Koppe, M.; Egelhaaf, H. J.; Dennler, G.; Scharber, M. C.; Brabec, C. J.; Schilinsky, P.; Hoth, C. N. Near IR Sensitization of Organic Bulk Heterojunction Solar Cells: Towards Optimization of The Spectral Response of Organic Solar Cells. *Adv. Funct. Mater.* **2010**, *20*, 338−346.

(18) Huang, J. S.; Goh, T.; Li, X.; Sfeir, M. Y.; Bielinski, E. A.; Tomasulo, S.; Lee, M. L.; Hazari, N.; Taylor, A. D. Polymer Bulk Heterojunction Solar Cells Employing Förster Resonance Energy Transfer. *Nat. Photonics* **2013**, *7*, 479−485.

(19) Wu, S.; Li, J.; Tai, Q.; Yan, F. Investigation of High-Performance Air-Processed Poly(3-Hexylthiophene)/Methanofullerene Bulk-Heterojunction Solar Cells. *J. Phys. Chem. C* **2010**, *114*, 21873−21877.

(20) Nam, C. Y.; Qin, Y.; Park, Y. S.; Hlaing, H.; Lu, X.; Ocko, B. M.; Black, C. T.; Grubbs, R. B. Photo-Cross-Linkable Azide-Functionalized Polythiophene for Thermally Stable Bulk Heterojunction Solar Cells. *Macromolecules* **2012**, *45*, 2338−2347.

(21) Zimmerman, J. D.; Xiao, X.; Renshaw, C. K.; Wang, S.; Diev, V. V.; Thompson, M. E.; Forrest, S. R. Independent Control of Bulk and Interfacial Morphologies of Small Molecular Weight Organic Heterojunction Solar Cells. *Nano Lett.* **2012**, *12*, 4366−4371.

(22) Della Pelle, A. M.; Homnick, P. J.; Bae, Y.; Lahti, P. M.; Thayumanavan, S. Effect of Substituents on Optical Properties and Charge-Carrier Polarity of Squaraine Dyes. *J. Phys. Chem. C* **2014**, *118*, 1793−1799.

(23) Nardes, A. M.; Ayzner, A. L.; Hammond, S. R.; Ferguson, A. J.; Schwartz, B. J.; Kopidakis, N. Photoinduced Charge Carrier Generation and Decay in Sequentially Deposited Polymer/Fullerene Layers: Bulk Heterojunction vs Planar Interface. *J. Phys. Chem. C* **2012**, *116*, 7293−7305.

(24) Schlenker, C. W.; Barlier, V. S.; Chin, S. W.; Whited, M. T.; McAnally, R. E.; Forrest, S. R.; Thompson, M. E. Cascade Organic Solar Cells. *Chem. Mater.* **2011**, *23*, 4132−4140.

(25) Sim, M.; Kim, J. S.; Shim, C.; Cho, K. Cascade Organic Solar Cells with Energy-Level-Matched Three Photon-Harvesting Layers. *Chem. Phys. Lett.* **2013**, *557*, 88−91.

(26) Sista, S.; Yao, Y.; Yang, Y.; Tang, M. L.; Bao, Z. Enhancement in open circuit voltage through a cascade-type energy band structure. *Appl. Phys. Lett.* **2007**, *91*, 223508.

(27) Tan, Z. K.; Johnson, K.; Vaynzof, Y.; Bakulin, A. A.; Chua, L. L.; Ho, P. K. H.; Friend, R. H. Suppressing Recombination in Polymer Photovoltaic Devices via Energy-Level Cascades. *Adv. Mater.* **2013**, *25*, 4131−4138.